J Mater Sci: Mater Med (2007) 18:171–177
DOI 10.1007/s10856-006-0677-6

Age-hardening behavior of a low-gold dental alloy

L. G. Pan · J. N. Wang

Received: 29 November 2004 / Accepted: 21 October 2005

Abstract The age-hardening behaviors of a low gold dental alloy were studied by means of differential scanning calorimetry, hardness testing, X-ray diffraction, optical microscopy and transmission election microscopy. Two distinct hardening behaviors were found at two different aging temperatures. Age-hardening at 290°C was attributed to the formation of the metastable AuCuI′ ordered phase, and the gradual softening in the overaging stage resulted from the slow growth of this phase. The rapid increase in hardness in the early stage at 495°C was due to the precipitation of the metastable AuCuI′ or/and AuCuII′ ordered phases, and the rapid decrease in hardness in the overaging stage was a consequence of the growth of these phases and the loss of the coherency strain at the interface between the spindal-like AuCuI platelets and the matrix.

1 Introduction

Gold alloys, consisting of Au, Cu, Ag and minor additions such as Pt, Pd, Ir and Zn, have been widely used for fabrication of inlays, crowns, bridges, and other dental prostheses for many years [1]. Such alloys resist corrosion and possess enough hardness and strength to withstand the considerably high occlusive forces that are normally generated during mastication. In order to achieve this property, the cast dental alloy is initially solution-treated to obtain a disordered solid solution and then subjected to age-hardening heat treatment. In the first stage the alloy is heat treated at a temperature higher than its order-disorder phase transformation temperature (normally >650°C), and all the atoms randomly arrange their positions (disordered solid solution). Rapid quenching prevents the formation of an ordered arrangement of Au and Cu atoms. In the second stage, the age-hardening treatment is accomplished by allowing diffusion to take place to form ordered AuCu phases. However, overaging causes the separation of the phases into a Cu-rich and Ag-rich phase and the growth of ordered twins [2]. The separation of the phases induces not only the decrease of the mechanical properties such as hardness and strength but also the deterioration of the corrosion resistance of the alloy. Therefore, control of the age-hardening is important for the clinical utilization of the gold alloy.

It has been reported that the hardening mechanism of the ternary Au-Ag-Cu alloy is related to phase transformation, such as ordering, precipitation and spinodal decomposition [3–9]. However, in order for low gold alloys to have the required mechanical properties such as hardness, strength, elasticity and ductility, other elements are frequently added. Since the compositions of these alloys are far from the equiatomic ratios, their aging-hardening behavior and the related mechanism are still not well understood, and inconsistency exists in the literature. Tani et al. [10] investigated the commercial type IV dental casting gold alloy, and reported that the age-hardening was due to the introduction of coherency strain at the interface between the AuCuI′ platelet and the matrix. Udoh et al. [11, 12] showed that the hardening in an 18 carat gold commercial dental alloy was caused by the ordering of Au_3Cu. Kim et al. [13] illustrated that the age-hardening in a commercial low-carat Au-Ag-Cu-Pd alloy was related to the precipitation of the metastable AuCuI′ and equilibrium AuCuI ordered phases and spinodal decomposition.

The purpose of this study is to further understand the age-hardening behavior of an Au-Ag-Cu low gold dental alloy with small amounts of other elements. In particular, it is

L. G. Pan · J. N. Wang (✉)
School of Materials Science and Engineering, Shanghai Jiao Tong University, 1954 Huashan Road, Shanghai 200030, P. R. of China
e-mail: jnwang@mail.sjtu.edu.cn

shown that differential scanning calorimetry (DSC) can be used to determine the optimal aging temperature and two distinct age-hardening behaviors were observed at a low and a high temperature, respectively.

2 Experiments

The alloy used in the present study had a nominal composition of 56Au-24.5Ag-13Cu-5.2Pd-0.7Zn-0.5Pt-0.1Ir (wt%). It was prepared by arc-melting with a non-consumable electrode in an argon atmosphere from constituent metals of better than 99.95% purity. To improve homogeneity, the alloy was melted four times and cast into an ingot. This was first solution treated at 700°C for 30 min and then quenched in ice water prior to heat treatment.

For DSC from room temperature to 650°C, a specimen of 300 mg was cut from the solution-treated ingot. The DSC experiment was performed at a heating rate of 10°C min^{-1} under a nitrogen atmosphere using a DSC-5p tester. For age-hardening, plate specimens of the size of 10 × 10 × 1.0 mm^3 were cut also from the solution-treated ingot. These specimens were annealed at two different temperatures for various periods of time. The annealing temperatures were selected to correspond to the exothermic peaks observed on the DSC curve. Hardness testing was carried out on the annealed samples using a Vickers hardness tester (Hv-50) with a load of 5 kg and a dwell time of 20 s. The average values of five indentations were taken as the Vickers hardness (Hv5) according to the methods of American Dental Associations specification No. 5 (ADA No. 5).

For X-ray diffraction (XRD) studies, solid specimens of the same size as those for the hardness testing were prepared, and analysed using an X-ray diffractometer (Dmax-rC) operated at 40 kV and 100 mA with nickel filtered Cu K_α radiation. For optical microscopic examination, plate specimens were polished using Al_2O_3 slurries and chemically etched with a freshly prepared aqueous solution consisting of 3 ml HCl, 9 ml HNO_3 and 1 ml glycerin. For transmission electron microscopic (TEM) observation, sheet specimens of about 80-μm thicknesses were first prepared. Discs of 3 mm diameter were then punched from them. These discs were electro-polished at 10°C by a double jet technique in a solution containing 35 g CrO_3, 200 ml CH_3COOH and 10 ml distilled water.

3 Results

3.1 Age-hardening

Figure 1 shows a typical DSC curve obtained by heating the solution-treated specimen from room temperature to 650°C.

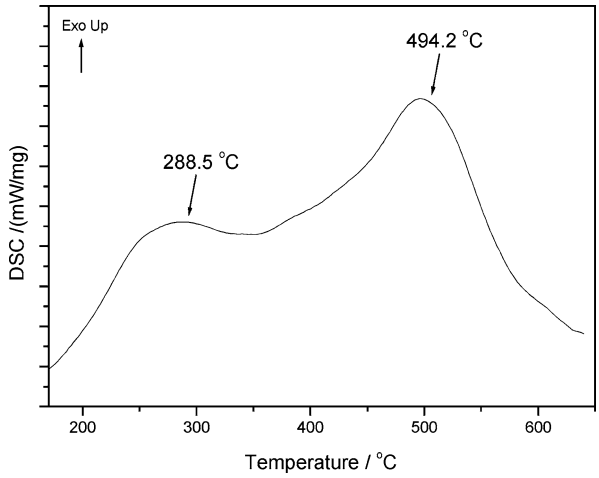

Fig. 1 DSC curve of the solution-treated specimen from room temperature to 650°C, and the heating rate was 10°C min^{-1}.

Two distinct exothermic peaks at 288.5°C and 494.2°C were observed, indicating two types of phase transformation. Therefore, isothermal aging was performed at both temperatures. Figure 2 demonstrates the variation of hardness with time for the samples aged at these two temperatures. As can be seen, there are generally three stages for each temperature. They are under-aging, peak-aging and over-aging. However, the detailed behaviors are different in the three stages at different temperatures. Notably, in the under-aging stage, age-hardening was much faster and reached the maximum much earlier at 495°C than at 290°C. In the peak-aging stage, the hardness level was slightly lower at 495°C than at 290°C. And in the over-aging stage, the hardness decreased much faster at 495°C than at 290°C.

To confirm that maximum hardening took place at the temperatures corresponding to the exothermic peaks on the DSC curve, traditional isochronal aging experiments were also

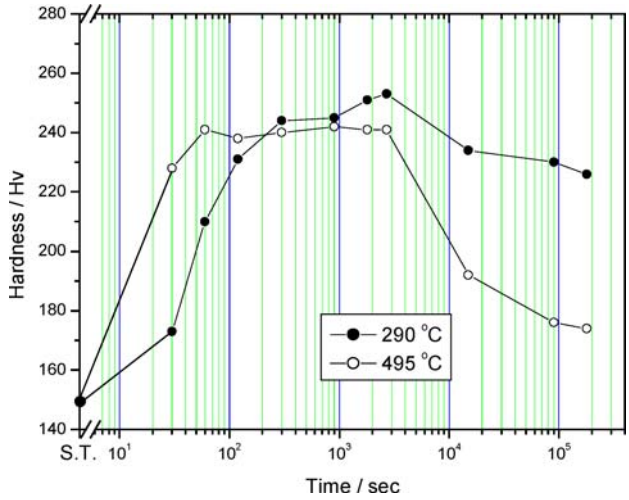

Fig. 2 Isothermal age-hardening curves at 290 and 495°C for various periods

conducted. They covered a temperature range from 200°C to 600°C for two aging times of 5 min and 15 min (Fig. 3). The isochronal age-hardening curves also show two clear hardness peaks, one at about 300°C and the other at 450–500°C. This behavior is consistent with that based on the DSC curve, and similar to those found for the type-IV and type-III dental gold alloys [12, 13].

3.2 X-ray diffraction

XRD was done to elucidate the phase transformation during the isothermal aging. Figure 4 shows the different XRD profiles for samples without aging and with aging at 290°C for three different periods (i.e., 2 min, 45 min, 2500 min). These aging periods corresponds to the three different aging stages (under-aging, peak-aging, and over-aging). The solution-treated specimen without aging revealed an α_0 single phase having a face-centered cubic (f.c.c.) structure. By aging up to 2.5×10^3 min, intensity of 111 and 200 reflections from the α_0 phase decreased and diffused, and 111 and 200 diffraction peaks shifted slightly toward low diffraction angles. For example the 111 diffraction angle (2θ) changed from 39.38° for the sample without aging to 38.96° for that with aging for 2.5×10^3 min.

Figure 5 shows the XRD profiles for the aging cases at 495°C. With aging, occurrence of superlattice reflections are visible, the metastable AuCuI′ with an f.c.t. structure and AuCuI′ with long-rang ordering were detected, and the 111 diffraction peak of the α_0 phase split into two phases. After aging for 2.5×10^3 min, the intensities of the coexisting phases of AuCuI and AuCuII increased. The space between the peak positions of the 1,1−1/2M,0 and 1,1 + 1/2M,0 superlattices became slightly wider, indicating that the antiphase domain size in the AuCuII superlattice, M, decreased with increasing aging time in the present alloy. The XRD

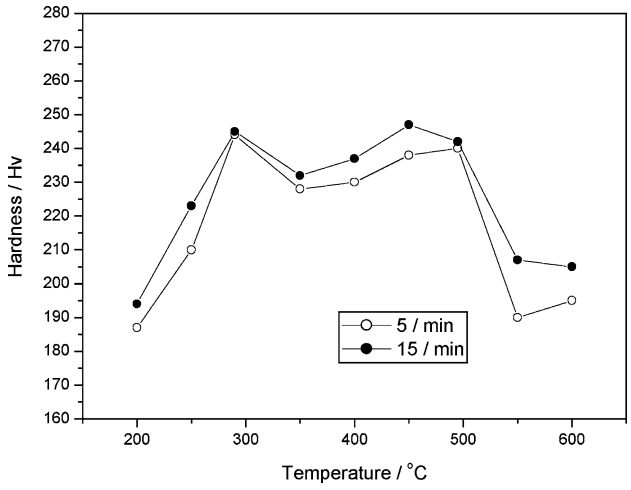

Fig. 3 Isochronal age-hardening curves for 5 and 15 min

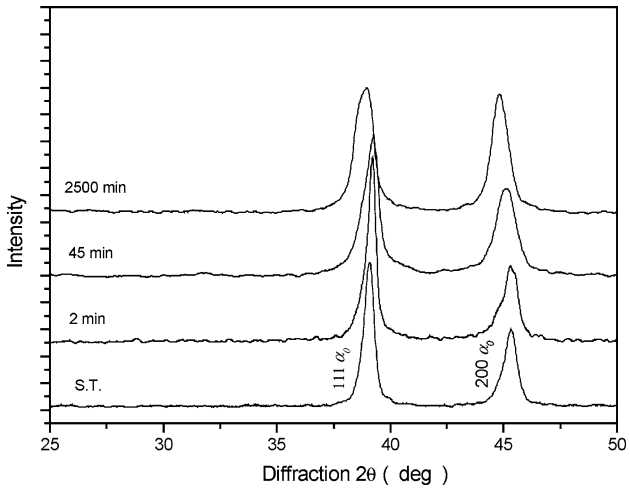

Fig. 4 X-ray diffraction patterns of the solution-treated specimens at 700°C for 30 min, and then aged at 290°C for various periods

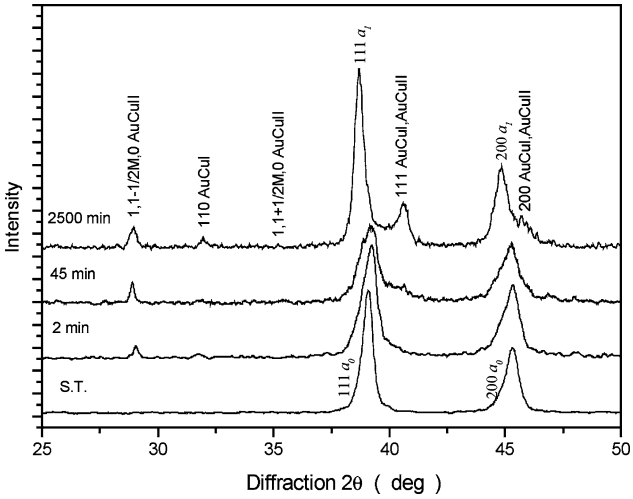

Fig. 5 X-ray diffraction patterns of the solution-treated specimens at 700°C for 30 min, and then aged at 495°C for various periods

results clearly suggests that the hardness of the specimen reached a maximum value in the very early stage due to the phase transformation from the α_0 phase to the metastable AuCuI′ or AuCuII′ phase as well as the α_1 (Ag-rich) phase.

3.3 Microstructure

After the samples were aged at 290°C for different periods, the only microstructure feature that was visible under optical microscope was nodular precipitates predominantly formed along the grain boundaries (Fig. 6). But when the samples were aged at 495°C, a lamellar structure was observed. Such structure formed at both grain boundaries and interiors. With increasing the aging time, the lamellar structure tended to expand and grow into the grain interior (Fig. 7).

Figure 8 shows the bright-field TEM image of the specimen aged at 290°C for 45 min. A high density of fine

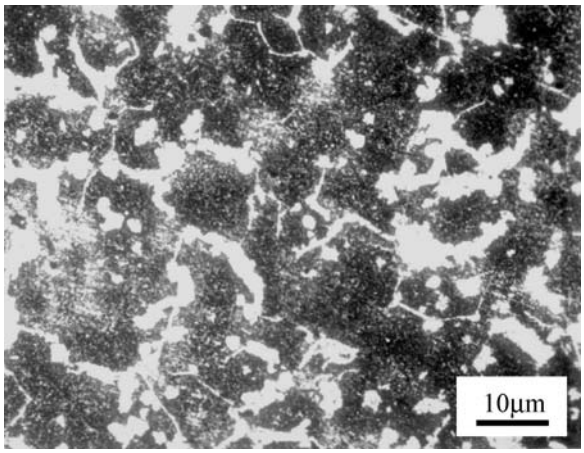

Fig. 6 Optical micrographs of the specimen aged at 290°C for 2.5×10^3 min

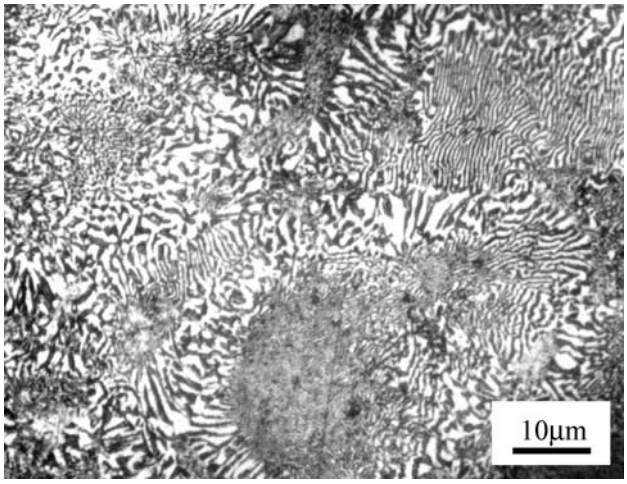

Fig. 7 Optical micrographs of the specimen aged at 495°C for 2.5×10^3 min

platelet-like precipitates can be seen to have formed parallel to the {100} plane. These fine precipitates are the f.c.t. metastable phase of AuCuI′. The axial ratio of this superlattice phase was determined from the SAED pattern (Fig. 8b) to be approximately 0.955. Figure 9 illustrates the bright-field TEM image of the specimen aged at 290°C for 2.5×10^3 min. By prolonged aging, it can be seen that the ordered platelets have grown in both their length and thickness. The growth rate of the AuCuI ordered platelets, however, seems very slow during aging at this temperature. The c/a axial ratio of the grown phase was determined to be approximately 0.926 as shown in Fig. 8d. Such result indicates that this phase is the ordered domains of AuCuI with an f.c.t structure that were nucleated and grown on the matrix {100} planes.

Figure 10 shows the bright-field TEM image of the specimen aged at 495°C for 45 min. Spindle-shaped precipitates of two orientations formed on {100} planes with the axis of the tetragonal AuCuI perpendicular to the *c* axis of the {100} plane. The two sets of precipitates made a right angle to each other. TEM examination revealed that there was a large coherent strain field at the interface between the AuCuI′ ordered platelets and the surrounding matrix. Figure 11 shows the bright-field TEM images of the specimen aged at 495°C for 2.5×10^3 min. Compared with that shown in Fig. 10a, the two sets of platelets have grown in their length and became slightly inclined to each other. Additionally, the coherent strain field observed in the 45 min sample disappeared at the interface between the platelets and the surrounding matrix.

4 Discussion

The DSC curve shown in Fig. 1 exhibits two exothermic peaks, and this observation indicates that two different stages of phase transformation are taking place. From the XRD and TEM studies, it can be noted that the exothermic peak at 290°C is attributable to the successive transitions from α_0 to Ag-rich α_1 and AuCuI ordered phase, and the exothermic peak at 490°C to the transformation from α_0 to Ag-rich α_1, AuCuI with an f.c.t. structure or/and AuCuI with long-range ordering.

4.1 Age-hardening behavior at 290°C

In an Au-Cu binary alloy with an equiatomic composition, there is a tendency for AuCuI with an ordered structure to form. It was reported that the AuCu ordered phase with a low degree of tetragonality could be produced easily in the

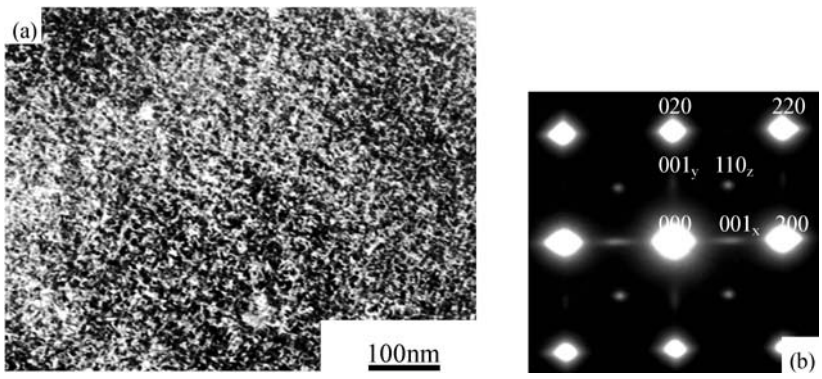

Fig. 8 The bright-field TEM image (a) and the SAED pattern (b) of the specimen aged at 290°C for 45 min

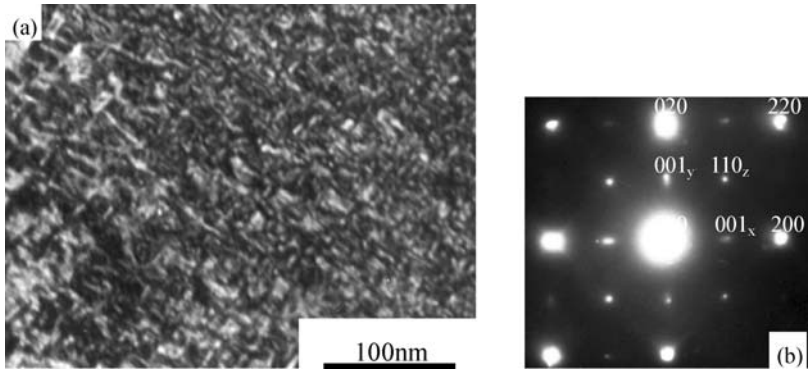

Fig. 9 The bright-field TEM image (a) and the SAED pattern (b) of the specimen aged at 290°C for 2.5×10^3 min

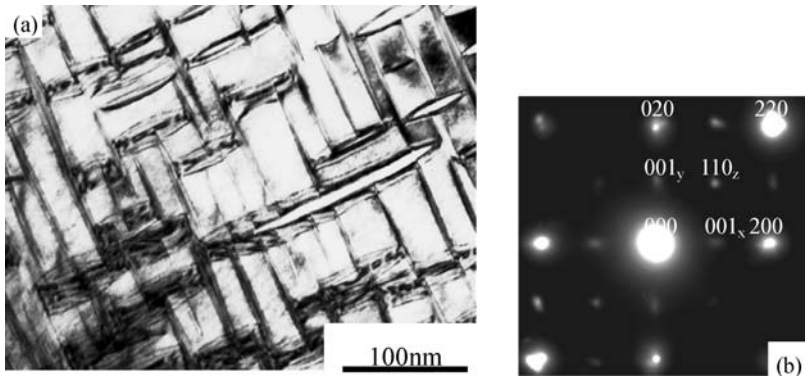

Fig. 10 The bright-field TEM image (a) and the SAED pattern (b) of the specimen aged at 495°C for 45 min

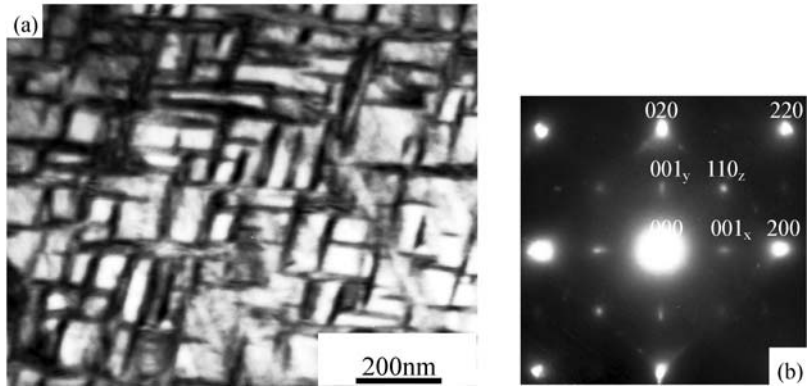

Fig. 11 The bright-field TEM image (a) and the SAED pattern (b) of the specimen aged at 495°C for 2.5×10^3 min

matrix f.c.c. phase [15]. But for commercial low-gold content alloys, at present, it is not clear which sites are occupied by other additions such as Ag, Pd and Pt. In fact, the structure properties of these alloys are influenced by the chemical site selectivity and the kind of substituents on the host site. Pd and Pt play a specially important role in the strengthening of dental gold alloys [16–18].

Tani et al. [10] and Hisatsune et al. [16] investigated the age hardening of commercial type IV dental casting gold alloys, and reported that the formation of a metastable ordered phase of the AuCuI′ type within grains contributed to the hardening. Kim et al. [14] studied the age-hardening reactions in a type III dental gold alloy and a commercial dental low-carat Au-Ag-Cu-Pd alloy, and concluded that the hardening was attributed to the formation of metastable AuCuI′ and equilibrium AuCuI ordered phases in the grain interior. Such kinds of transformation resulting hardening were also observed in the present alloy aged at 290°C.

The isothermal age-hardening curve of the present alloy aged at 290°C shows three stages of hardening. But at the optical microscopic scale, no apparent microstructural changes were observed. After 2.5×10^3 min of aging, a number of nodular precipitates appeared along the grain boundary (Fig. 6). On the other hand, based on the XRD study, 111 and 200 diffraction peaks shifted toward the low diffraction angle, and the lattice parameter of a_0 changed from 0.3961 nm to 0.4001 nm correspondingly. Such peaks suggest a silver-rich (α_1) phase with an f.c.c. structure.

TEM observation and SAED studies were made in order to elucidate the structure changes, as shown in Fig. 8. Fine precipitate platelets were visible along {100} planes of the disordered matrix (Fig. 8a), and the 001_x, 001_y, 110_z superlattice spots were found in the SAED pattern (Fig. 8b). These platelet precipitates were identified as the metastable AuCuI′ ordered phase with an f.c.t. lattice. The axial ratio c/a of the AuCuI′ phase was determined to be approximately 0.955.

Since an ordered phase with a low degree of tetragonality can be produced easily in the matrix f.c.c. phase, it may be concluded that the hardening at the initial stage of aging is attributed to the precipitation of the metastable AuCuI′ ordered platelets on the {100} planes of the disordered matrix. When this precipitation takes place, a considerable amount of strain may be introduced since a structure change from an f.c.c. to f.c.t. lattice is involved.

With increasing aging time, the ordered structure developed and formed platelets along the matrix {100} plane (Fig. 9a). The striations along the {100} directions disappeared (Fig. 9b), and the axial ratio (c/a) of these platelets was found to be 0.926. This observation suggests that the platelet-like ordered phases were transformed from the metastable AuCuI′ ordered phase to the equilibrium AuCuI ordered phase with an f.c.t. structure. However, the growth rate of the AuCuI′ ordered platelets appeared to be very slow at this aging temperature of 290°C.

4.2 Age-hardening behavior at 495°C

When the specimens were aged at 495°C, the isothermal age-hardening curves exhibited rapid hardening at the initial stage, slight stagnation at the maximum hardness, and then rapid softening. Although a considerable increase in hardness was observed at the initial stage of aging, there was no apparent microstructural change within 100 min at the optical microscopic scale. However, further aging resulted in the lamellar structure growing into nodule products along the grain boundaries, and a fine fingerprint-like lamellar structure began to form in the grain interior, as shown in Fig. 7. It is obvious that the softening is, at least partially, due to the coarsening of the nodules products and the fine lamellar structure.

The XRD results (Fig. 5) show that the 1,1 ± 1/2M,0 and 110 superlattice reflections are visible at the initial stage of aging. Here, M represents the periodic-antiphase-domain size. The superlattices formed at this temperature were identified as metastable the AuCuI′ with an f.c.t. structure and AuCuII′ with long-range ordering. The lattice parameters of the AuCuI ordered phase were determined to be $a = 0.3978$ nm, $c = 0.3606$, and $c/a = 0.906$. This is consistent with the TEM result shown in Fig. 11, which also suggests the formation a modulated structure composed of the Ag-rich α_1 and AuCuI′ with an f.c.t. structure. From the change in XRD pattern and microstructure, it may be concluded that the hardening was attributed to the precipitation of the coexisting phases (AuCuI′ and AuCuII′) from the α_0 disordered solid solution. The axial ratio of this ordered phase was determined to be approximately 0.918 by SAED patterns in Fig. 11b.

Spindle-like platelets and thin strap-like platelets were found on the disordered matrix {100} planes with their c-axes perpendicular to each other, as shown in Fig. 10(a). It was also found that there was a strain field at the interface between the spindle-like platelets and the surrounding matrix along the {100} direction. With further aging, the strain field surrounding the spindle-like platelets disappeared, and these thin platelets had grown in both their length and thickness (Fig. 11a). At the same time, the angle between the spindle-like and the thin strap-like platelets changed from 90° to 102°. Such change might result in the observed loss of the coherency strain around the AuCuI platelets, and thus the decrease in hardness in the overaging stage.

5 Conclusions

The age-hardening behaviors and associated phase transformation in a low gold dental alloy were studied by means of DSC, hardness testing, XRD, optical microscopy, and TEM. The following conclusions may be made:

1. DSC can be used for determination of the aging temperature for optimal hardening. The result is consistent with that obtained from the traditional isochronal aging experiments.
2. Two different hardening behaviors can be distinguished in the present alloy. They can be observed at the two optimal hardening temperatures of 290°C and 495°C.
3. The hardening at 290°C is a result of the transition from α_0 to α_1 (Ag-rich) and AuCuI with an f.c.t. structure, and the gradual softening at the overaging stage is due to the slow growth of the thin metastable AuCuI′ platelets along the {100} direction in the disordered matrix.
4. The hardening at 495°C is a consequence of the transition from α_0 to α_1, AuCuI or/and AuCuII. The drastic decrease in hardness in the overaging stage is caused by the coarsening of the AuCu phases and the loss of coherency strain at the interface between the AuCuI′ ordered phase and the matrix.

References

1. R. W. PHILLIPS, Skinner's Science of Dental Materials (W. B. Sauners Co., Philadelphia, 1982), p. 374.

2. M. OHTA, T. SHIRAISHI, M. YAMANE and K. YASUDA, *Dent. Mater. J.* **2** (1983) 10.
3. K. HISATSUNE, K. UDOH, B. I SOSROSOEDIRDJO, T. TANI and K. YASUDA, *J. Alloys Compd.* **176** (1991) 269.
4. M. NAKAGAWA and K. YASUDA, *J. Mater. Sci.* **23** (1988) 2975.
5. P. SKJERPE, J. GJONNES, E. SORBRODEN and H. HERO, *J. Mater. Sci.* **21** (1986) 3986.
6. K. YASUDA, M. NAKAGAWA, G. V. TENDELOO and S. AMELINCKX, *J. Less-Common Mat.* **135** (1987) 169.
7. M. NAKAGAWA and K. YASUDA, *J. Less-Common Mat.* **138** (1988) 95.
8. K. UDOH, K. YASUDA G. V. TENDELOO and J. V. LANDUYT, *J. Alloys Compd.* **176** (1991) 147.
9. K. UDOH, H. FUJIYAMA, K, HISATSUNE, M. HASAKA and K. YASUDA, *J. Mater. Sci.* **27** (1992) 504.
10. T. TANI, K. UDOH, K. YASUDA, G. V. TENDELOO and J. V. LANDUYT, *J. Dent. Res.* **70** (1991) 1350.
11. K. UDOH, K. YASUDA and M. OHTA, *J. Less-Common Met.* **118** (1986) 249.
12. K. HISATUNE, K. UDOH, M. NAKAGAWA and M. HASAKA, *J. Less-Common Mat.* **160** (1990) 247.
13. H. I. KIM, M. I. JANG and B. J. JEON, *J. Mater. Sci.: Mater. Med.* **8** (1997) 333.
14. H. I. KIM, Y. K. KIM, M. I. JANG, K. HISATSUNE and A. A. E. S. SAKRANA, *Biomater.* **22** (2001) 433.
15. K. HISTSUNE, Y. TANAKA, K. UDOH and K. YASUDA, *Intermetallics* **3** (1995) 335.
16. K. HISATSUNE, M. NAKAGAWA, K. UDOH and B. SOSROSOEDIRDJO, *J. Mater. Sci.: Mater. Med.* **1** (1990) 49.
17. A. PRASAD, T. J. ENG and K. MUKHERJEE, *Mater. Sci. Eng.* **43** (1976) 179 .
18. K. YASUDA and M. OHTA, *J. Dent. Res.* **61** (1982) 473.